

Short communication

Beatrice Severino*, Ferdinando Fiorino, Angela Corvino, Giuseppe Caliendo, Vincenzo Santagada, Diego Magno Assis, Juliana R. Oliveira, Luiz Juliano, Serena Manganelli, Emilio Benfenati, Francesco Frecentese, Elisa Perissutti and Maria Aparecida Juliano

Synthesis, biological evaluation, and docking studies of PAR2-AP-derived pseudopeptides as inhibitors of kallikrein 5 and 6

Abstract: A series of protease activated receptor 2 activating peptide (PAR2-AP) derivatives (**1–15**) were designed and synthesized. The obtained compounds were tested on a panel of human kallikreins (hK1, hK2, hK5, hK6, and hK7) and were found completely inactive toward hK1, hK2, and hK7. Aiming to investigate the mode of interaction between the most interesting compounds and the selected hKs, docking studies were performed. The described compounds distinguish the different human tissue kallikreins with compounds **1** and **5** as the best hK5 and hK6 inhibitors, respectively.

Keywords: human kallikrein 5; human kallikrein 6; inhibitor; molecular modeling; serine protease.

DOI 10.1515/hsz-2014-0190

Received April 22, 2014; accepted July 25, 2014; previously published online July 31, 2014

Human kallikreins (hKs) are a multigene family of 15 secreted serine-type proteases (Yousef et al., 2000; Yousef and Diamandis, 2001). Kallikrein-related peptidases show a high degree of homology with trypsin; this similarity is related both to the primary structure and to the catalytic

mechanism. All but four kallikrein-related peptidases present an Asp residue homologous to that of trypsin, located at the base of the substrate-binding pocket, addressing the specificity toward positively charged Lys and Arg residues. Human tissue kallikrein 5 (hK5), first isolated from human plantar stratum corneum (Brattsand and Egelrud, 1999), is found in many tissues and it appears to be most abundantly expressed in human skin (Shaw and Diamandis, 2007). hK5 was reported to play role in a kallikrein proteolytic cascade pathway activating the prostate kallikreins hK2 and hK3 that participate in seminal clot liquefaction and possibly in prostate cancer progression (Michael et al., 2006). Moreover, hK5 can play a major role in the pathobiology of Netherton syndrome (NS), a rare genetic skin disease (Hovnanian, 2012). hK5 has a trypsin-like specificity, with a strong preference for Arg over Lys residues at P1 position of the substrates. The specificities of the other subsites were not determined in detail; however, the S2 subsite seems to accept hydrophobic amino acids as Pro and Phe (Michael et al., 2005; Debela et al., 2006).

A number of hKs are expressed in the central nervous system (CNS); among them, hK6 is the most studied and its involvement in several neurodegenerative diseases such as Alzheimer's disease, Parkinson's disease, and multiple sclerosis has been documented (Diamandis et al., 2000; Ogawa et al., 2000). A detailed analysis of hK6 substrate specificity showed that it is a restricted arginyl hydrolase and has high preference for hydrophobic amino acids at P2 and P1' positions (Angelo et al., 2006). On the basis of this study, the best substrate thus far reported for hK6 was synthesized, Abz-AFR↓FSQ-EDDnp, which was cleaved at the R-F bond (as indicated by ↓). It is noteworthy that the AFRFS sequence was found as a motif in the amino-terminal domain of seven human ionotropic glutamate receptor subunits. It has been suggested that hK1 and hK6 are directly implicated in

***Corresponding author: Beatrice Severino**, Dipartimento di Farmacia, Università degli Studi di Napoli 'Federico II', Via D. Montesano, 49, I-80131 Napoli, Italy, e-mail: bseverin@unina.it
Ferdinando Fiorino, Angela Corvino, Giuseppe Caliendo, Vincenzo Santagada, Francesco Frecentese and Elisa Perissutti: Dipartimento di Farmacia, Università degli Studi di Napoli 'Federico II', Via D. Montesano, 49, I-80131 Napoli, Italy

Diego Magno Assis, Juliana R. Oliveira, Luiz Juliano and Maria Aparecida Juliano: Departamento de Biofísica, Escola Paulista de Medicina, Universidade Federal de São Paulo, Rua Três de Maio 100, São Paulo 04044-020, Brasil

Serena Manganelli and Emilio Benfenati: IRCCS, Istituto di Ricerche Farmacologiche Mario Negri, Via La Masa 19, I-20156 Milano, Italy

neurodegeneration and could be useful tools to follow multiple sclerosis progression (Scarlsbrick et al., 2008).

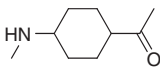
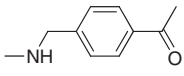
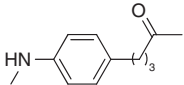
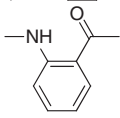
Aside from their involvement in pathologies of the skin and CNS, overexpression of hKLK5 and hKLK6 occurs in several malignancies, including ovarian, breast and testicular cancer. Accumulating evidence suggests that hKLKs are activators of protease activated receptors (PARs) that comprise four G protein-coupled receptors (PAR1, PAR2, PAR3, and PAR4) (Caliendo et al., 2012). It has been reported that hKLK5, through PAR2 signaling, increases the expression of proinflammatory cytokines and chemokines in human primary keratinocytes (Briot et al., 2009); hKLK6 evoked intracellular Ca^{2+} flux mediated by PAR1 in neurons and both PAR1 and PAR2 in astrocytes (Vandell et al., 2008). Moreover, a study on the substrate specificity of hKLK6, performed using fluorescence resonance energy transfer peptides derived from sequences that span the cleavage sites for activation of PAR1–4, has shown that only the substrate with the PAR2 sequence was hydrolyzed (Angelo et al., 2006).

hKLK5 and hKLK6 inhibitors would be very useful pharmacological tools for elucidating the physio-pathological processes where the mentioned kallikrein isoforms are involved; moreover, these inhibitors might serve as lead compounds for developing new drugs to treat diseases that result from their uncontrolled activities. The development of hKLK6 inhibitors is thus far scarce, although hKLK6 is involved in neurodegenerative diseases and cancer. A series of *N*-(4-aminomethylphenyl)-2-hydroxy-benzamide derivatives have been recently reported, and the most potent inhibitor presented a K_i of 0.3 μM (Liang et al., 2012a). Some natural isocoumarins, instead, have shown their ability in inhibiting hKLK5 and hKLK7, with vioxanthin being the most potent inhibitor toward hKLK5 with $K_i=22.9 \mu\text{M}$ (Teixeira et al., 2011).

Starting from the consideration that PAR2 is a hKLK5 and hKLK6 substrate, we hypothesize that compounds derived from the PAR2 activating peptide (PAR2-AP), namely the sequence SLIGRL, could be prepared and assayed for activity against hKLK5 and hKLK6. Moreover, to verify their selectivity toward other hKLKs, the compounds were tested also toward hKLK1, hKLK2, and hKLK7.

Compounds 1–4 were already described in a previous article reporting a SAR study on PAR2-AP derivatives obtained replacing Ile³-Gly⁴ dipeptide backbone with more rigid difunctional scaffolds (Santagada et al., 2002). Compounds 5–15 are lower molecular weight (MW) derivatives in which an aliphatic or aromatic nucleus, variously substituted, has been linked to the PAR2-AP carboxy-terminal dipeptide Arg-Leu. The structures of the compounds are reported in Tables 1 and 2. Compounds 1–15

Table 1 Chemical data for compounds 1–4.

NH ₂ -Ser-Leu --- SPACER --- Arg-Leu-NH ₂				
Compd	SPACER	t_R (min)	MW	
			Calcd	Found
1		19.17	611.8	613.0
2		17.22	619.8	620.6
3		25.22	647.8	648.7
4		21.84	605.7	606.6

Compounds 1–15 were synthesized by SPPS using the standard Fmoc method in a manual reaction vessel and in a stepwise fashion. For each compound, 0.5 g (0.35 mequiv) of Rink amide MBHA resin was used. Each Fmoc-amino acid was coupled in a 3-fold excess, through TBTU/HOBt/DIPEA, except for the first amino acid that was used in a 5-fold excess and coupled through DIPCDI/HOBt. The Fmoc protecting groups were removed by treatment with a 25% piperidine in DMF (45 min). The commercially available difunctional scaffolds *cis*-4-aminocyclohexanecarboxylic acid, 4-(aminomethyl)benzoic acid, 4-(4-aminophenyl)butanoic acid, *trans*-4-(aminomethyl)cyclohexanecarboxylic acid, 2-aminobenzoic acid, and 4-aminobenzoic acid were dissolved in 9% Na_2CO_3 and converted to the corresponding Fmoc derivatives by treatment with a solution of *N*-(9-fluorenylmethoxycarbonyloxy)succinimide (Fmoc-OSu) in DMF. Each protected pseudopeptide was cleaved from the resin, and the amino acid side chains were simultaneously deprotected by treatment with a mixture of TFA/DCM/TIS/anisole (90:5:3:2) for 2 h at room temperature under nitrogen atmosphere. The conditions employed for purification and characterization of the pseudopeptides are reported in Table 2.

were synthesized by Fmoc solid-phase peptide synthesis (SPPS). Mature hKLK1, hKLK2, hKLK5, hKLK6, and hKLK7 were expressed and purified from baculovirus/insect cell line system as previously described (Bernett et al., 2002). The compounds presented in Tables 1 and 2 were completely inactive toward hKLK1 and hKLK2, which also have a high preference for Arg at the cleavage site, and were also inactive on hKLK7, which has a high specificity for Phe and Tyr. As shown in Table 3, several of the described compounds display interesting K_i values toward hKLK5 and/or hKLK6. Therefore, these compounds distinguish the different human tissue kallikreins. The compounds of the series NH₂-S-L-spacer-R-L-NH₂ (1–4) were more effective inhibitors for hKLK5 (K_i values ranging from 1.0±0.05 to 31±2 μM) than for hKLK6 (K_i values ranging from 2.9±0.2 to 254±20 μM). In contrast, the compounds

Table 2 Chemical data for compounds 5–15.

Spacer --- Arg-Leu-NH ₂				
Compd	Spacer	t _R (min)	MW	
			Calcd	Found
5		18.54	424.9	425.8
6		16.04	425.6	426.5
7		19.26	396.5	397.7
8		22.80	474.5	475.3
9		18.38	426.5	427.8
10		22.30	458.5	459.6
11		14.09	405.5	406.3
12		16.97	447.6	448.5
13		24.07	390.5	391.4
14		14.21	419.5	420.8
15		20.88	396.5	397.4

The crude compounds were purified by reversed phase (RP)-HPLC on a preparative Vydac C18 column (15–20 μm, 50×250 mm; The Separations Group, Inc., Hesperia, CA, USA) using a gradient of CH₃CN in 0.1% aqueous TFA (from 0% to 45% in 35 min) at a flow rate of 30 ml/min. Analytical RP-HPLC was done using the following conditions: RP Vydac C18 column (5 μm, 4.6×250 mm) and a two-solvent system: eluent A, 0.05% TFA (v/v) in water; eluent B, 0.05% TFA (v/v) in acetonitrile; eluted in a linear gradient from 0% to 50% B during 35 min, UV detection at 220 nm, and flow rate at 1 ml/min. Analytical RP-HPLC indicated a purity of >98%, and the correct MWs were confirmed by electrospray ionization-MS, performed on a ThermoFinnigan LCQ Ion-Trap mass spectrometer (Thermo Fisher Scientific Inc., Waltham, MA, USA).

of the series spacer-R-L-NH₂ (5–15) were less effective inhibitors for hKLK5, with **12** and **13** as the best inhibitors of the series, which, in contrast, are very poorly effective toward hKLK6. The best inhibitors for hKLK6 in the series

Table 3 K_i values toward hKLK5 and hKLK6, respectively, of compounds 1–15 and the lowest ΔG docking values of the most significant clusters of hKLK5 and hKLK6 complexed with compounds 1, 2, 5, and 7.

Compd	hKLK5		hKLK6	
	K _i (μM)	ΔG (kcal/mol)	K _i (μM)	ΔG (kcal/mol)
1	1.0±0.05	-7.29	2.9±0.2	-8.13
2	1.2±0.07	-6.8; -6.2	4.4±0.3	-9.54
3	2.9±0.1	–	45±3	–
4	31±2	–	254±20	–
5	Not inhibited	-8.44 ^a ; -7.38 ^a	1.5±0.08	-8.62; -8.36
6	9.0±0.6	–	3.9±0.2	–
7	Not inhibited	-8.97 ^a	5.7±0.3	-8.30
8	15±1	–	8.4±0.6	–
9	21±2	–	13.0±0.8	–
10	43.0±5	–	21.8±2	–
11	38±2	–	26.3±3	–
12	4.9±0.4	–	26.3±2	–
13	4.3±0.3	–	77±6	–
14	11.9±0.9	–	148±8	–
15	Not inhibited	–	178±13	–

Assays were carried out at 37°C in 50 mM Tris/HCl and 1 mM EDTA (pH 9.0). The substrate used was 5.3 μM Abz-KLRSSQ-EDDnp (K_m=2.9 μM and K_{cat}=14.7 s⁻¹; enzyme concentration, 2 nM). The K_i values were calculated using the relations v₀/v_i=1+[I]/K_i(app), where v₀ is the hydrolysis velocity in the absence of inhibitors and v_i is the velocity in the presence of different concentrations of the inhibitors. K_i values were obtained using the relation K_i=K_i(app)/(1+[S]/K_m). Mature hKLK1, hKLK2, hKLK5, hKLK6, and hKLK7 were expressed and purified from baculovirus/insect cell line system, as previously described (Bernett et al., 2002). The final yield of purified mature hKLKs was typically 20–25 mg/l of culture. The purity of mature hKLKs was assessed by SDS-PAGE (w/v 15% polyacrylamide gel) and Coomassie brilliant blue staining, N-terminal sequencing, and MALDI-TOF MS. The protein samples were about 98% homogeneous, with no visible degradation products and had the expected mature N-terminus corresponding to the mature proteases. Molar concentrations of active hKLK6 and hKLK1 were determined by titration with 4-methylumbelliferyl p-guanidinobenzoate hydrochloride by spectrofluorimetric titration as described previously (Jameson et al., 1973).

^aThese ΔG values refer to the different binding modes supposed to be responsible for the lack of inhibition of these compounds.

NH₂-S-L-spacer-R-L-NH₂ incorporated both flexible (**1**) as well as rigid spacers (**2**). However, the most rigid structure, as compound **4**, reduced the inhibition by two orders of magnitude. The lower inhibition activity of compound **3** compared with that of **2** indicated that the length of the spacer has significant influence on the interaction with hKLK6.

Aiming to investigate the mode of interaction between the most interesting compounds and the selected hKLKs, docking studies were performed. To verify the presence of direct and frequent interactions between some PAR2-AP

derivatives and, respectively, hKLK5 and hKLK6, molecular docking with Autodock v4.2 was performed. Compounds **1**, **2**, **5**, and **7** were considered the most significant, as they all inhibited hKLK6, while, tested on hKLK5, the first two chemicals showed the lowest experimental K_i values and the last two had no inhibition activity. The two proteases and the assayed compounds were considered as rigid receptors and flexible ligands, respectively. At first, the flexible ligands were designed with Marvin Sketch v5.10, followed by the investigation of the lowest energy conformer within the force field MMFF94. At the same time, the crystal-bound structures of hKLK5 and hKLK6 complexed with their inhibitors, leupeptin and 4-[[[(3R)-3-[[[(7-methoxynaphthalen-2-yl)sulfonyl](thiophen-3-ylmethyl)amino]-2-oxopyrrolidin-1-yl]methyl]thiophene-2-carboximidamide, respectively (Liang et al., 2012b), were downloaded as .pdb files (2PSX and 3VFE) from the Protein Data Bank and visualized to define their specific binding sites.

Two grids of proper sizes centered on these identified portions were built. Their associated parameter values were specific for each hKLK. Coordinates (x , y , and z) of the center of the grid of the two hKLKs were chosen on the basis of the crystal structure of the protease-ligand complex. This choice was made considering the protein binding sites, keeping the fundamental amino acids for interactions and also in line with the dimensions of the ligands to be docked.

Moreover, genetic algorithm (GA) was selected as the docking mode. GAs are a class of optimization methods that are based on various computational models of Darwinian evolution (Goldberg, 1989) (the term 'evolutionary algorithms' is also used to describe such methods). GAs involve the creation of a population of potential solutions that gradually evolves toward better solutions, and the use of a chromosome to encode each member of the population. In these methods, each chromosome in a population encodes one conformation of the ligand together with its orientation within the binding site. A scoring function is used to calculate the fitness of each member of the population and to select individuals for each iteration. As with the Monte Carlo search methods, the underlying random nature of the GA means that it is usual to perform a number of runs and to select the structures with the highest scores (Leach and Gillet, 2007). GA was combined with a method of local search, providing a hybrid algorithm, named Lamarckian GA.

The reliability of a docking result depends on the energies of the docked structures found at the end of each run and on their similarities to each other. In Autodock, the similarity of docked structures is measured by computing the root-mean-square deviation (rmsd) between

the coordinates of the atoms. One way to measure the reliability of a result is to compare the rmsd of the lowest energy conformations and their rmsd to one another, to group them into families of similar conformations (clusters). In this process, the lowest energy conformation is used as the seed for the first cluster. Next, the second conformation is compared with the first. If it is within the rmsd tolerance, it is added to the first cluster. If not, it becomes the first member of a new cluster. This process is repeated with the rest of the docked results, grouping them into families of similar conformations. In this work, different clusters were made and examined at different rms tolerance values until 3.5 Å was chosen as the most proper value for grouping. Before making this choice for the synthesized compounds, the originally bound structures were redocked for the calibration. Using an rmsd tolerance of 2.0 Å, a cluster analysis is automatically performed by Autodock. The lowest binding energy cluster of redocked leupeptin and 4-[[[(3R)-3-[[[(7-methoxynaphthalen-2-yl)sulfonyl](thiophen-3-ylmethyl)amino]-2-oxopyrrolidin-1-yl]methyl]thiophene-2-carboximidamide) was consistent with their crystallographic poses, and they had minimum free binding energy values of -7.93 and -9.68 kcal/mol, respectively.

The docking scores in Autodock are provided by ΔG binding values. Outputting structurally similar clusters are ranked by Autodock in order of increasing energy. Thus, the lowest binding energy value cluster is assigned to the cluster rank 1. The ranking of the ligands was correct for all the docked compounds, and their free binding energy range values were consistent with those of the original inhibitors.

Compound **1** had the highest torsional degree of freedom owing to the coexistence of four amino acid free side chains and a cyclohexane moiety in its two lowest energy chair conformations. These two main structural features let these derivatives accommodate in different ways. Thus, clusters of similar docked poses were poorly populated, and the output was slightly ambiguous. However, in the complexes with the lowest binding energy, the Arg side chain extended to the S1 pocket, and its carbonyl group was in close contact with Ser195 O γ or Gly193, thus resembling the P1-Arg3i of leupeptin with its terminal carbonyl group and the amidinothiophene group of 4-[[[(3R)-3-[[[(7-methoxynaphthalen-2-yl)sulfonyl](thiophen-3-ylmethyl)amino]-2-oxopyrrolidin-1-yl]methyl]thiophene-2-carboximidamide, respectively (Figure 1). Moreover, a high degree of superposition turned out for these Arg residues in the lowest energy docked structures of **1** with the positively charged moieties current in the relative cocrystallized ligands (Figure 2).

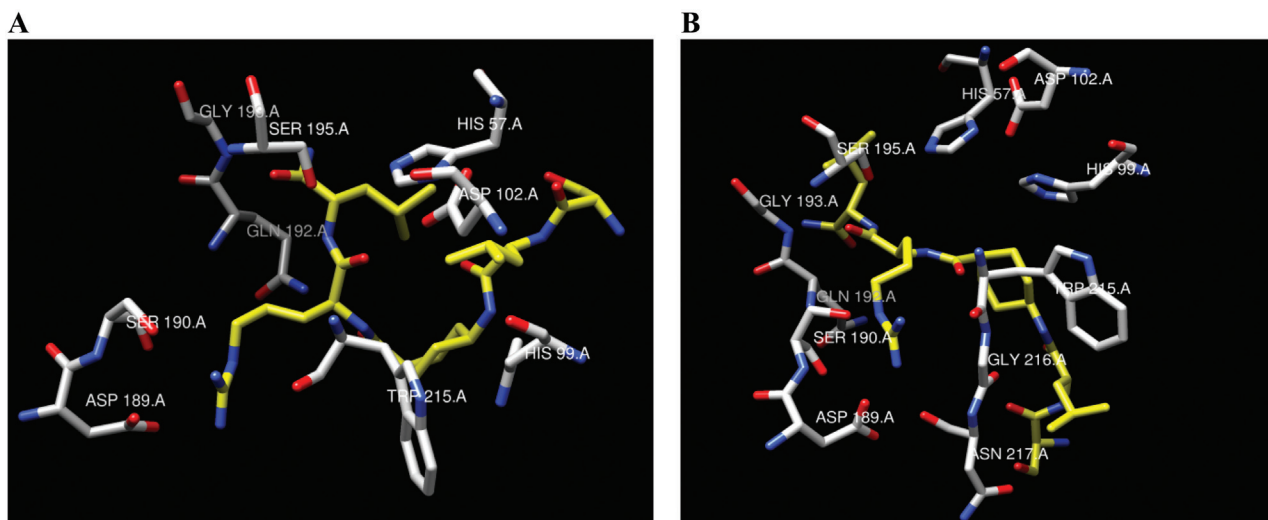


Figure 1 (A) Compound 1 in the hKLLK5 substrate binding site, where the carbon atom of compound 1 are in yellow and those of hKLLK5 are in light gray. (B) Compound 1 in the hKLLK6 substrate binding sites, where the carbon atoms of compound 1 are in yellow and those of hKLLK6 are in light gray. Docking studies: compounds 1–15 were designed with Marvin Sketch v5.10, followed by the investigation of the lowest energy conformer within the force field MMFF94. The visualization was performed with UCSF Chimera v1.7. Molecular docking was done with Autodock v4.2, using the following protocol for both hKLLK5 and hKLLK6: genetic algorithm (GA); number of GA runs: 100; population size: 150; maximum number of evaluations: long (25 000 000); other parameters set with their default values. To address the ligand on the supposed binding site, Autogrid 4 was performed, selecting the following parameters for hKLLK5: number of points in x-dimension: 50; number of points in y-dimension: 48; number of points in z-dimension: 40; spacing: 0.375 (default); center grid box (x, y, z): 6.566, -2.509, 20.503. For hKLLK6, Autogrid 4 was performed, keeping the same number of points in x, y, and z dimensions and the same spacing, but the following center grid box (x, y, z): -3.087, -10.988, -16.074.

In general, all the supposed inhibitors kept this binding mode. Thus, it may be considered responsible for the lack of proteolytic activity or at least strictly related to it. The lowest free binding energy values for compound 1 complexed with hKLLK5 and hKLLK6 were -7.29 and -8.13 kcal/mol, respectively.

Compound 2 showed this conservative orientation of Arg residue both in the lowest binding energy

cluster and in the largest cluster complexes with hKLLK5 (Figure 3). The relative free binding energy ranges were 1.05 kcal/mol (minimum=-6.8 kcal/mol) and 3.81 kcal/mol (minimum=-6.2 kcal/mol), respectively.

In the first mentioned complex, the CO of the aromatic spacer was in close contact with the $N\epsilon^2$ atom of Gln192 and its hydrophobic benzene ring was partially aligned with the P2-Leu2i side chain of the leupeptin crystallographic

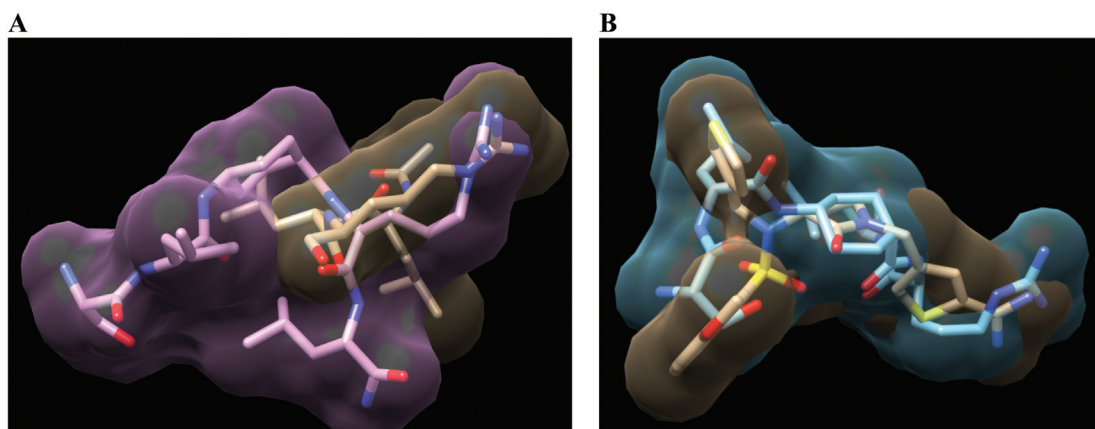


Figure 2 Superposition of compound 1 with crystallographic poses of leupeptin (A) and 4-[[[(3R)-3-[[[(7-methoxynaphthalen-2-yl) sulfonyl] (thiophen-3-ylmethyl) amino]-2-oxopyrrolidin-1-yl] methyl] thiophene-2-carboximidamide (B). The carbon atoms of leupeptin and amidinothiophene derivative are in light gray, while those of compound 1 are in purple (A) and cyan (B), respectively.

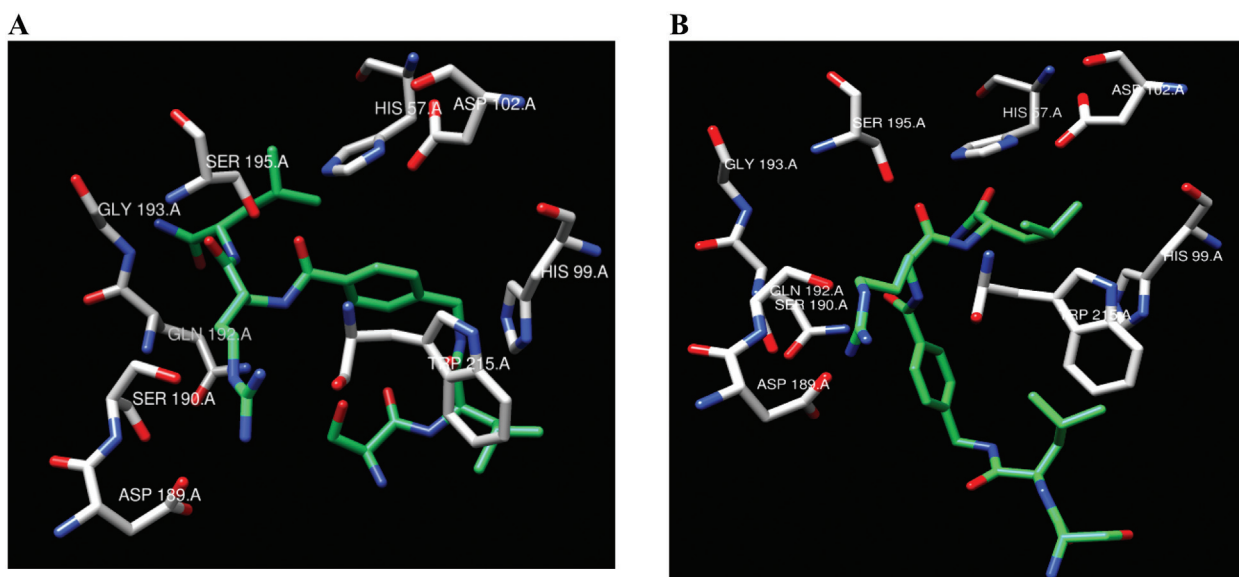


Figure 3 The lowest energy complex of the lowest binding energy cluster (A) and of the largest cluster (B) complexes of compound **2** in the hKLK5 substrate binding site.

The carbon atoms of compound **2** are in sea green and those of hKLK5 are in light gray.

pose. In the second one, the spacer was superposed on the P3-Leu1 residue, while the C-terminal Leu was on the P2-Leu2i residue of leupeptin. For hKLK6, 25 analogous complexes with compound **2** were obtained in the lowest binding energy cluster that was also the most populated one, with a ΔG range of 4.94 kcal/mol (minimum=-9.54 kcal/mol).

Two similar main clusters were fed by 22 and 19 docked structures of compound **5** complexed with hKLK6, respectively. The ΔG range values were 2.27 kcal/mol (minimum=-8.62 kcal/mol) and 1.23 kcal/mol

(minimum=-8.36 kcal/mol). The Arg side chain extends into S1 resembling the amidinothiophene group, in close contact with the carboxylic side chain of Asp189 and the backbone carbonyl oxygen of Asn217, while the Leu side chain is situated adjacent to Ser195, simulating the pyrrolidinone group. On the other hand, frequently *p*-chlorophenyl group slots into the S4 cleft, delimited by Trp215, which is free in the crystallographic pose (Figure 4). However, the specificity in S4 for hydrophobic residues follows the order hKLK4>hKLK5>hKLK6>hKLK7 (non-specific), which means that this pocket in hKLK6 can

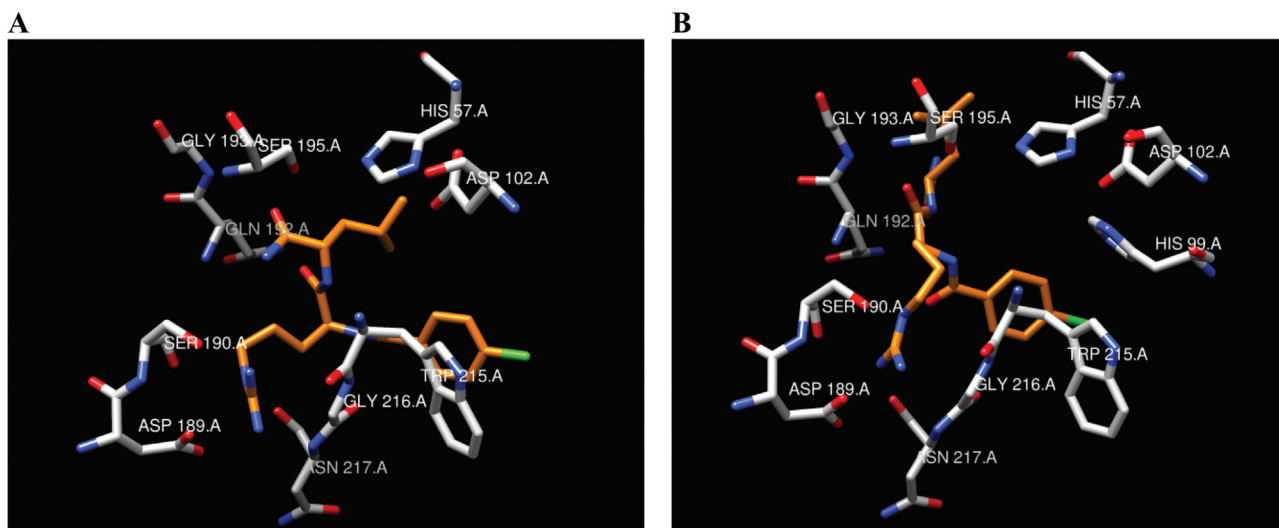


Figure 4 The lowest energy cluster (A) and the largest cluster (B) complexes of compound **5** in the hKLK6 substrate binding site.

The carbon atoms of compound **5** are in orange and those of hKLK6 are in light gray.

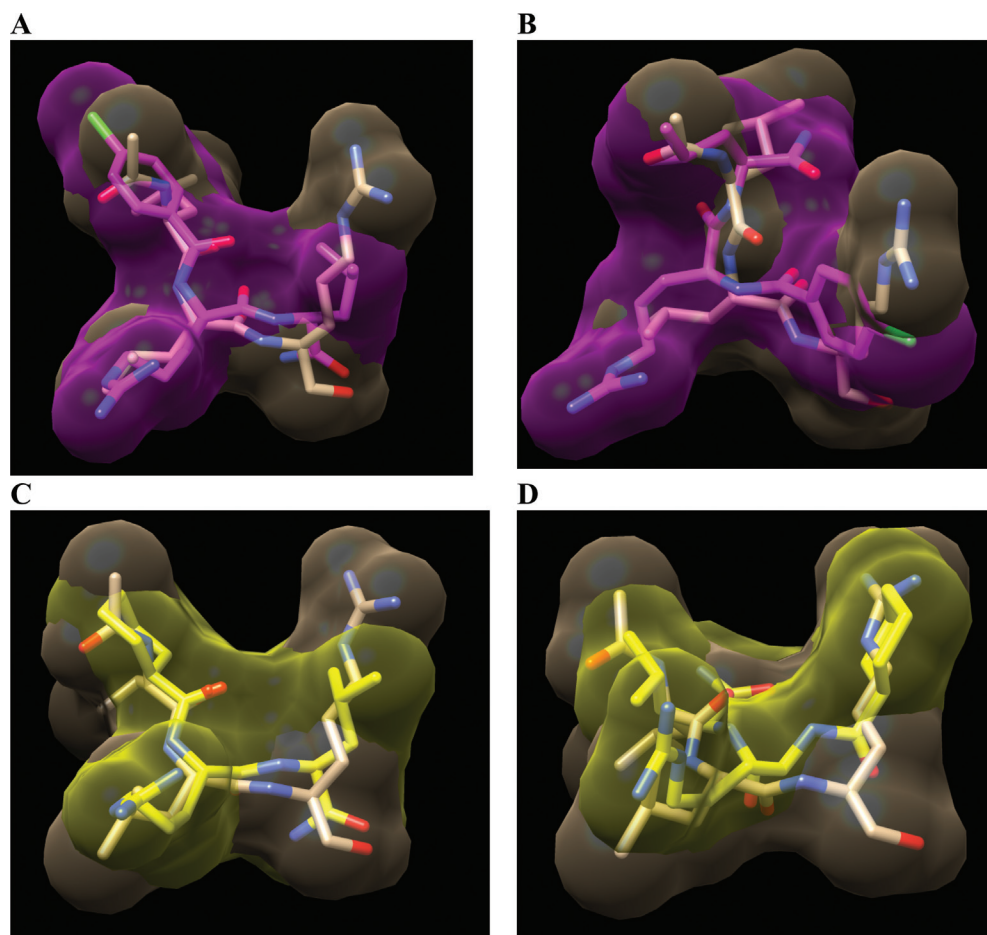


Figure 5 Superposition of crystallographic poses of leupeptin with compounds **5** (A and B) and **7** (C and D).

The carbon atoms of leupeptin are in light gray and those of compounds **5** and **7** are in magenta and yellow, respectively. The hydrophobic spacers of the two non-inhibitors could be aligned with the opposite moiety in leupeptin.

accommodate any non-polar group (Debela et al. 2008). These conformations were visible in the results of the alignment process with the crystallized inhibitor. In contrast, a completely opposite orientation with the Arg side chain extending into the catalytic triad was kept by compound **5** docked with hKLL5 in the most significant cluster. This chain could not be aligned with the leupeptin correspondent one, but only matches with the hydrophobic Leu residues were allowed (Figure 5A,B). Thus, this different binding mode and an incorrect alignment with cocrystallized leupeptin were supposed to be responsible for the lack of inhibition in the docking output with hKLL5 for both compounds **5** and **7** (Figure 5C,D). For these two compounds, the interactions with Asp189 were replaced by that with Asp102 of the catalytic triad. Even if compound **7** docked with hKLL6 showed two different main poses and not only that seen thus far to be related to the inhibition activity, the overall results supported the hypothesis of an inhibition mechanism based on the binding mode and

suggested a correlation between specific conformations and activities.

In conclusion, the PAR2-AP derivatives **1–15** have been prepared and tested for their ability to inhibit a panel of hKs. The compounds were able to distinguish the different hKLLs acting as inhibitors only toward hKLL5 and hKLL6. Compound **1** ($K_i=1.0\pm 0.05\ \mu\text{M}$) was the most effective toward hKLL5, while **5** ($K_i=1.5\pm 0.08\ \mu\text{M}$), besides being the best hKLL6 inhibitor, was also very selective, being completely inactive toward all the other hKLLs tested in our study. The promising results here obtained indicate these new compounds as valid leads for further optimization studies aiming to improve the potency of this new class of hKLL5 and hKLL6 inhibitors.

Acknowledgments: This work was supported by Fundação de Amparo à Pesquisa do Estado de São Paulo (FAPESP – project-12/50191-4R), Conselho Nacional de Desenvolvimento Científico e Tecnológico (CNPq – projects 471340/2011-1 and 470388/2010-2).

References

- Angelo, P.F., Lima, A.R., Alves, F.M., Blaber, S.I., Scarisbrick I.A., Blaber, M., Juliano, L., and Juliano, M.A. (2006). Substrate specificity of human kallikrein 6: salt and glycosaminoglycan activation effects. *J. Biol. Chem.* *281*, 3116–3126.
- Bennett, M.J., Blaber, S.I., Scarisbrick, I.A., Dhanarajan, P., Thompson, S.M., and Blaber, M. (2002). Crystal structure and biochemical characterization of human kallikrein 6 reveals that a trypsin-like kallikrein is expressed in the central nervous system. *J. Biol. Chem.* *277*, 24562–24570.
- Brattsand, M. and Egelrud, T. (1999). Purification, molecular cloning, and expression of a human stratum corneum trypsin-like serine protease with possible function in desquamation. *J. Biol. Chem.* *274*, 30033–30040.
- Briot, A., Deraison, C., Lacroix, M., Bonnart, C., Robin, A., Besson, C., Dubus, P., and Hovnanian, A. (2009). Kallikrein 5 induces atopic dermatitis-like lesions through PAR2-mediated thymic stromal lymphopoietin expression in Netherton syndrome. *J. Exp. Med.* *206*, 1135–1147.
- Caliendo, G., Santagada, V., Perissutti, E., Severino, B., Fiorino, F., Frecentese, F., and Juliano, L. (2012). Kallikrein protease activated receptor (PAR) axis: an attractive target for drug development. *J. Med. Chem.* *55*, 6669–6686.
- Debela, M., Magdolen, V., Schechter, N., Valachova, M., Lottspeich, F., Craik, C.S., Choe, Y., Bode, W., and Goettig, P. (2006). Specificity profiling of seven human tissue kallikreins reveals individual subsite preferences. *J. Biol. Chem.* *281*, 25678–25688.
- Debela, M., Beaufort, N., Magdolen, V., Schechter, N.M., Craik, C.S., Schmitt, M., Bode, W., and Goettig, P. (2008). Structures and specificity of the human kallikrein-related peptidases KLK 4, 5, 6, and 7. *Biol. Chem.* *389*, 623–632.
- Diamandis, E.P., Yousef, G.M., Petraki, C., and Soosaipillai, A.R. (2000). Human kallikrein 6 as a biomarker of Alzheimer's disease. *Clin. Biochem.* *33*, 663–667.
- Goldberg D.E. (1989). *Genetic Algorithms in Search, Optimization, and Machine Learning* (Reading, MA: Addison-Wesley).
- Hovnanian, A. (2012). Netherton syndrome: new advances in the clinic, disease mechanism and treatment. *Exp. Rev. Dermatol.* *7*, 81–92.
- Jameson, G.W., Roberts, D.V., Adams, R.W., Kyle, W.S.A., and Elmore, D.T. (1973). Determination of the operational molarity of solutions of bovine α -chymotrypsin, trypsin, thrombin and factor Xa by spectrofluorimetric titration. *Biochem. J.* *131*, 107–117.
- Leach, A.R. and Gillet, V.J. (2007). *An Introduction to Chemoinformatics* (Dordrecht, the Netherlands: Springer).
- Liang, G., Chen, X., Aldous, S., Pu, S.F., Mehdi, S., Powers, E., Xia, T., and Wang, R. (2012a). Human kallikrein 6 inhibitors with a *para*-amidobenzylaniline P1 group identified through virtual screening. *Bioorg. Med. Chem. Lett.* *22*, 2450–2455.
- Liang, G., Chen, X., Aldous, S., Pu, S.F., Mehdi, S., Powers, E., Giovanni, A., Kongsamut, S., Xia, T., Zhang, Y., et al. (2012b). Virtual screening and X-ray crystallography for human kallikrein 6 inhibitors with an amidinothiophene P1 group. *ACS Med. Chem. Lett.* *3*, 159–164.
- Michael, I.P., Sotiropoulou, G., Pampalakis, G., Magklara, A., Ghosh, M., Wasney, G., and Diamandis, E.P. (2005). Biochemical and enzymatic characterization of human kallikrein 5 (hK5), a novel serine protease potentially involved in cancer progression. *J. Biol. Chem.* *280*, 14628–14635.
- Michael, I.P., Pampalakis, G., Mikolajczyk, S.D., Malm, J., Sotiropoulou, G., and Diamandis, E.P. (2006). Human tissue kallikrein 5 is a member of a proteolytic cascade pathway involved in seminal clot liquefaction and potentially in prostate cancer progression. *J. Biol. Chem.* *281*, 12743–12750.
- Ogawa, K., Yamada, T., Tsujikawa, Y., Taguchi, J., Takahashi, M., Tsuboi, Y., Fujino, Y., Nakajima, M., Yamamoto, T., Akatsu, H., et al. (2000). Localization of a novel type trypsin-like serine protease, neurosin, in brain tissues of Alzheimer's disease and Parkinson's disease. *Psychiatry Clin. Neurosci.* *54*, 419–426.
- Santagada, V., Caliendo, G., Severino, B., Perissutti, E., Fiorino, F., Cicala, C., De Filippis, V., and Cirino, G. (2002). Minimal structural requirements for agonist activity of PAR-2 activating peptides. *Bioorg. Med. Chem. Lett.* *12*, 21–24.
- Scarisbrick, I.A., Linbo, R., Vandell, A.G., Keegan, M., Blaber, S.I., Blaber, M., Sneve, D., Lucchinetti, C.F., Rodriguez, M., and Diamandis, E.P. (2008). Kallikreins are associated with secondary progressive multiple sclerosis and promote neurodegeneration. *Biol. Chem.* *389*, 739–745.
- Shaw, J.L.V. and Diamandis, E.P. (2007). Distribution of 15 human kallikreins in tissues and biological fluids. *Clin. Chem.* *53*, 1423–1432.
- Teixeira, T.S.P., Freitas, R.F., Abrahao, Jr., A., Devienne, K.F., de Souza, L.R., Blaber, S.I., Blaber, M., Kondo, M.J., Juliano, M.A., Juliano, L., et al. (2011). Biological evaluation and docking studies of natural isocoumarins as inhibitors for human kallikrein 5 and 7. *Bioorg. Med. Chem. Lett.* *21*, 6112–6115.
- Vandell, A.G., Larson, N., Laxmikanthan, G., Panos, M., Blaber, S.I., Blaber, M., and Scarisbrick, I.A. (2008). Protease-activated receptor dependent and independent signaling by kallikreins 1 and 6 in CNS neuron and astroglial cell lines. *J. Neurochem.* *107*, 855–870.
- Yousef, G.M. and Diamandis, E.P. (2001). The new human tissue kallikrein gene family: structure, function, and association to disease. *Endocr. Rev.* *22*, 184–204.
- Yousef, G.M., Chang, A., Scorilas, A., and Diamandis, E.P. (2000). Genomic organization of the human kallikrein gene family on chromosome 19q13.3-q13.4. *Biochem. Biophys. Res. Commun.* *276*, 125–133.